Draft version February 5, 2024
Typeset using LaTeX twocolumn style in AASTeX631

The first quenched galaxies, when and how?

Lizhi Xie (谢利智)[1,2] Gabriella De Lucia[2,3] Fabio Fontanot[2,3] Michaela Hirschmann[4,2] Yannick M. Bahé[5] Michael L. Balogh[6] Adam Muzzin[7] Benedetta Vulcani[8] Devontae C. Baxter[9] Ben Forrest[10] Gillian Wilson[11] Gregory H. Rudnick[12] M. C. Cooper[13] and Umberto Rescigno[14,15]

[1] *Tianjin Normal University, Binshuixidao 393, Xiqing, 300387, Tianjin, China*
[2] *INAF Astronomical Observatory of Trieste, via G.B. Tiepolo 11, I-34143 Trieste, Italy*
[3] *IFPU - Institute for Fundamental Physics of the Universe, via Beirut 2, 34151, Trieste, Italy*
[4] *Institute for Physics, Laboratory for Galaxy Evolution and Spectral Modelling, Ecole Polytechnique Federale de Lausanne, Observatoire de Sauverny, Chemin Pegasi 51, CH-1290 Versoix, Switzerland*
[5] *Laboratory for Astrophysics, École Polytechnique Fédérale de Lausanne (EPFL), Observatoire de Sauverny, Chemin Pegasi 51, CH-1290 Versoix, Switzerland*
[6] *Department of Physics and Astronomy, University of Waterloo, Waterloo, Ontario N2L 3G1, Canada*
[7] *Department of Physics and Astronomy, York University, 4700 Keele St., Toronto, Ontario MJ3 1P3, Canada*
[8] *INAF- Osservatorio Astronomico di Padova, Vicolo Osservatorio 5, 35122 Padova, Italy*
[9] *Department of Astronomy & Astrophysics, University of California, San Diego, 9500 Gilman Dr, La Jolla, CA 92093, USA*
[10] *Department of Physics and Astronomy, University of California Davis, One Shields Avenue, Davis, CA 95616 USA*
[11] *Department of Physics, University of California Merced, 5200 Lake Road, Merced, CA 95353, USA*
[12] *Department of Physics and Astronomy, University of Kansas, Lawrence, KS 66045, USA*
[13] *Department of Physics and Astronomy, University of California, Irvine, 4129 Frederick Reines Hall, Irvine, CA 92697, USA*
[14] *Instituto de Astronomía y Ciencias Planetarias de Atacama (INCT), Universidad de Atacama, Copayapu 485, Copiapó, Chile*
[15] *Instituto de Astrofisica, Universidad Andres Bello, Fernandez Concha 700, Las Condes, Santiago RM, Chile*

ABSTRACT

Many quenched galaxies discovered in the early Universe by *JWST* raise fundemental question s on when and how these galaxies became quiescent. Making use of the latest version of the semi-analytic model GAEA that provides good agreement with the observed quenched fractions up to $z \sim 3$, we make predictions for the expected fractions of quiescent galaxies up to $z \sim 7$ and analyze the main quenching mechanism. We find that in a simulated box of 685 Mpc on a side, the first quenched massive ($M_\star \sim 10^{11}\mathrm{M}_\odot$), Milky Way mass, and low mass ($M_\star \sim 10^{9.5}\mathrm{M}_\odot$) galaxies appear at $z \sim 4.5$, $z \sim 6.2$, and before $z = 7$. Most quenched galaxies identified at early redshifts remain quenched for more than 1 Gyr. Independently of galaxy stellar mass, the dominant quenching mechanism at high redshift is accretion disk feedback (quasar winds) from a central massive black hole, which is triggered by mergers in massive and Milky Way mass galaxies, and by disk instabilities in low-mass galaxies. Environmental stripping become increasingly more important at lower redshift.

Keywords: Galaxy — Quenching — Simulation

1. INTRODUCTION

The cessation of star formation in galaxies has drawn considerable attention in recent years, especially given the large numbers of quiescent massive galaxies that have been found in the early Universe (Schreiber et al. 2018; Merlin et al. 2019; Girelli et al. 2019; Glazebrook et al. 2017; Nanayakkara et al. 2022), where the timescale available to assemble and quench these systems is short. Spectroscopic confirmation suggests that these galaxies experience short periods of intense star formation, grow up to $10^{11}\mathrm{M}_\odot$ in the first one or two billion years of the universe, and then stop forming stars within the next few million years (Forrest et al. 2020; Valentino et al. 2020; Kakimoto et al. 2023; Carnall

xielizhi.1988@gmail.com

et al. 2023a). This rapid assembly and quenching process might challenge our current understanding of galaxy formation (Finkelstein et al. 2023).

The number densities of quenched massive galaxies $M_\star > 10^{10.5}\mathrm{M}_\odot$ increase rapidly from $\sim 10^{-6}$ Mpc^{-3} at $z \sim 5$ to as much as a factor of 10 times higher at $z \sim 3$ (Marsan et al. 2022), although the measured number densities have a relatively large scatter due to different selection criteria and cosmic variance (Valentino et al. 2023). The classical UVJ color selection of quenched galaxies (Wuyts et al. 2008) is found to be incomplete and underestimates the number of quenched galaxies at $z > 3$ (Schreiber et al. 2018). Some studies favour a NUVrJ (Ilbert et al. 2013) or ugi color selection (Antwi-Danso et al. 2023) to identify galaxies that have been quenched recently, which is important for galaxies at $z > 3$ (Gould et al. 2023; Kubo et al. 2024).

Despite large scatter in measurements, it is a solid conclusion that most theoretical models under-predict the number densities of quenched galaxies (Cecchi et al. 2019; Girelli et al. 2019; Gould et al. 2023) at $z > 4$ by about an order of magnitude. Weaver et al. (2023) found that quenched galaxies in the SHARK model (Lagos et al. 2023) and IllustrisTNG simulation (Pillepich et al. 2018) at $3.5 < z < 4.5$ are not as massive as the observed ones. Either creating enough massive galaxies at early cosmic epochs or quenching them on a short time scale remains a challenge for current galaxy formation models.

Various physical mechanisms have been proposed to explain the rapid assembly of mass in the early Universe, including weaker feedback (Dekel et al. 2023), enhanced star formation efficiencies (Wang et al. 2023), and a top-heavy IMF (Trinca et al. 2023). The physical mechanisms driving quenching also remain unclear. Quenching could be caused by internal feedback from active galactic nuclei (AGN) and supernovae (SN) feedback, or by external physical processes including galaxy-galaxy interactions and environmental stripping. With a minimal physical model, Gelli et al. (2023) suggests that SN feedback is not powerful enough to quench galaxies of $\sim 10^8\mathrm{M}_\odot$ at high redshift. The fact that many high-z quenched galaxies are found to host luminous AGN (Ito et al. 2022; Shimakawa et al. 2023) suggests an important contribution to quenching from feedback from their central supermassive black holes (SMBH). This appears to be confirmed in recent theoretical works: Kurinchi-Vendhan et al. (2023) and Kimmig et al. (2023) analyze the massive quenched galaxies in TNG and Magneticum at $z \sim 3$ and show that these galaxies are indeed quenched by AGN feedback. Lovell et al. (2023) found the AGN feedback is the dominant quenching mechanism for galaxies above $10^9\mathrm{M}_\odot$ at $z \sim 5$. Qin et al. (2017) use semi-analytic models to identify analogs of quenched galaxies observed at $z \sim 5$ and show that these have grown through significant mergers and host the most massive black holes at their redshifts. Some quenched galaxies are found in over-dense environments (Kubo et al. 2021; McConachie et al. 2022; Tanaka et al. 2023; Alberts et al. 2023), suggesting environmental quenching may also contribute as early as $z \sim 4$.

In our recent work (De Lucia et al. 2024, here after GAEA2023), we present the latest version of our GAlaxy Evolution and Assembly (GAEA) model and show that it can correctly reproduce the observed quenched fractions up to redshift ~ 3 as well as the number densities of quenched galaxies up to redshift ~ 5, better than many state-of-the-art models and simulations. The good agreement with observations makes it a perfect tool for studying the physical origin of quenched galaxies at high redshift.

In this work, we extend the analysis presented in De Lucia et al. (2024) to the quenched fractions and their quenching mechanisms since $z \sim 7$. In Section 2, we introduce the semi-analytic model and our methodology. In Section 3 and Section 4, we present the results and give our conclusions.

2. MODEL AND SIMULATION

GAEA2023 (De Lucia et al. 2014) now combines independent versions of the model including an improved treatment for the supernovae feedback (Hirschmann et al. 2016), of the multi-phase cold gas (Xie et al. 2017), of environmental effects (Xie et al. 2020), and of AGN accretion and feedback (Fontanot et al. 2020). In particular, GAEA2023 implements a treatment for tidal stripping and ram pressure stripping that gradually removes hot gas, as well as ram-pressure stripping of cold gas, for satellite galaxies. These implementations help to solve the over-quenching of low-mass satellite galaxies and to improve the model predictions in terms of gas fractions (Xie et al. 2020). GAEA2023 also implements an updated modeling for cold gas accretion onto supermassive black holes. Mergers and disk instability cause a fraction of cold gas to lose angular momentum and flow towards the center, where it forms an accretion disk around the super massive black hole. This material is then accreted onto the SMBH on a viscous timescale: accretion can heat the surrounding gas and cause an outflow (for details about the model, we refer to Fontanot et al. 2020. Below, we refer to this process as accretion disk feedback. GAEA2023 has been calibrated to reproduce the galaxy stellar mass function up to $z \sim 3$, HI mass function and quenched fractions at

$z \sim 0$, as well as AGN luminosity function up to $z \sim 4$. In De Lucia et al. (2024) we show that this model version reproduces well the observed quenched fraction, as well as the stellar mass function of the quenched population up to $z \sim 3$. GAEA2023 is in good agreement with the observed quenched fraction, as well as the stellar mass function of the quenched population up to $z \sim 4$.

The model is run on the Millennium Simulation (Springel et al. 2005) with a box size of 685 Mpc based on a WMAP 1-yr cosmology (Spergel et al. 2003) with $\Omega_m = 0.25$, $\sigma_b = 0.045$, $\sigma_8 = 0.9$, and $h = 0.73$.

In the following, we will compare GAEA2023 results with predictions from TNG100 and TNG300 (Springel et al. 2018; Nelson et al. 2018; Naiman et al. 2018; Marinacci et al. 2018; Pillepich et al. 2018). The TNG project is a suite of cosmological magneto-hydro-dynamical simulations, adopting the Planck cosmology (Planck Collaboration et al. 2016) with $\Omega_m = 0.3089$, $\Omega_b = 0.0486$, $\sigma_8 = 0.8159$, and $h = 0.6774$. The TNG100 and TNG300 have model cubic boxes of side length approximately 100 and 300 Mpc. TNG considers two modes of AGN feedback: for high accretion rates, the surrounding gas is heated by thermal feedback from AGN. When the accretion rates are low, gas instead receive a kinetic 'kick' that causes gas outflows. In this work, we use the publicly available database to retrieve the simulated stellar mass, star formation rate, and black hole mass within twice the stellar half-mass radius.

3. RESULTS

3.1. *Quenched fraction*

Figure 1 shows the evolution of quenched fractions as predicted by GAEA2023 for low-mass ($2 - 4 \times 10^9 \mathrm{M}_\odot$), Milky-Way-mass ($2 - 4 \times 10^{10} \mathrm{M}_\odot$), and massive galaxies ($0.8 - 1.5 \times 10^{11} \mathrm{M}_\odot$). We consider different defintions for quenched galaxies: first, we select a sample imposing specific star formation rate $sSFR = SFR/M_\star < 0.3/t_H$, where t_H is the Hubble time at given redshift (Franx et al. 2008). Then in order to get a fair comparison with observational data, we also present quenched fractions based on a UVJ (synthetic) color selection. We tried different cuts commonly adopted in the literature (Williams et al. 2009; Whitaker et al. 2011; Muzzin et al. 2013; Martis et al. 2016) and plot the scatter obtained as shaded regions in Fig. 1. The error boxes show observational measurements of quenched fractions for galaxies from the UltraVISTA DR1 and 3D-HST surveys (Martis et al. 2016). In the redshift range $0 < z < 3$, there is a good agreement between GAEA2023 and data at all mass scales. The quenched fraction defined using the synthetic UVJ photometry are similar to those defined by sSFR at $z < 2$, but decrease more rapidly at $z > 2$. As for GAEA2023, the UVJ color selection fails to find significant numbers of quiescent galaxies at $z > 2$. For TNG the quenched fractions of galaxies with $M_\star \sim 10^{11} \mathrm{M}_\odot$ are larger than observational measurement.

Moving to higher redshifts, the predicted quenched fractions decrease. In the framework of GAEA2023, the quenched fraction of low-mass galaxies is 0.2 per cent at $z \sim 7.3$, *i.e.* 6 out of 2880 galaxies are quenched. The quenched fraction remains below 1 per cent until $z \sim 3$. We traced 42 quenched low-mass galaxies at $z \sim 6.2$ forward in time and found that 11 of them move back to the main sequence within 0.5 Gyr. Most of the high-redshift quenched low-mass galaxies, however, remain quiescent for more than 1 Gyr, indicating they are not just temporarily quenched between two episodes of bursty star formation.

The first quenched galaxies with mass similar to the Milky Way appear at $z \sim 6.2$, *i.e.* 2 out of 116 Milky Way-like galaxies are quenched. One of these two returns to the main sequence after ~ 0.5 Gyr. The other is a satellite that remains quenched until it merges with another galaxy. The quenched fraction, for galaxies of this mass, grows quickly to 10 per cent between $4 < z < 5$.

The first massive quenched galaxies (with $M_\star \sim 10^{11} \mathrm{M}_\odot$) are found at $z \sim 4.5$. 2 out of 35 galaxies in this mass bin are quenched at this redshift. In the subsequent evolution, these two galaxy continue to have a low star formation rate for most of the time. We have tested low cut $sSFR < 10^{-11}$ yr^{-1} to define quiescent galaxies and find our results do not depend significantly on the SFR cut adopted.

Predictions from TNG are quite different from those based on GAEA2023, with systematically lower quenched fractions at high redshift, and no quenched galaxy at $z > 4$. It is in clear tension with the observed fact of spectroscopically confirmed quenched massive galaxies at $z > 4$(e.g. Carnall et al. 2023b). A similar result is reported in Merlin et al. (2019), where a lower sSFR cut 10^{-11} yr^{-1} was used. Though most massive galaxies at $z \sim 4$ have a central massive black hole of $10^8 \mathrm{M}_\odot$, only a minor fraction of them are quenched. In TNG, kinetic feedback from AGN represents the most efficient quenching mechanism for massive galaxies (Kurinchi-Vendhan et al. 2023). However, the accretion rates at high redshift are so large that the assumed mode for AGN feedback in TNG comes in the form of thermal feedback, which is not efficient enough to quench galaxies at $z > 3$.

3.2. *Quenching Mechanisms*

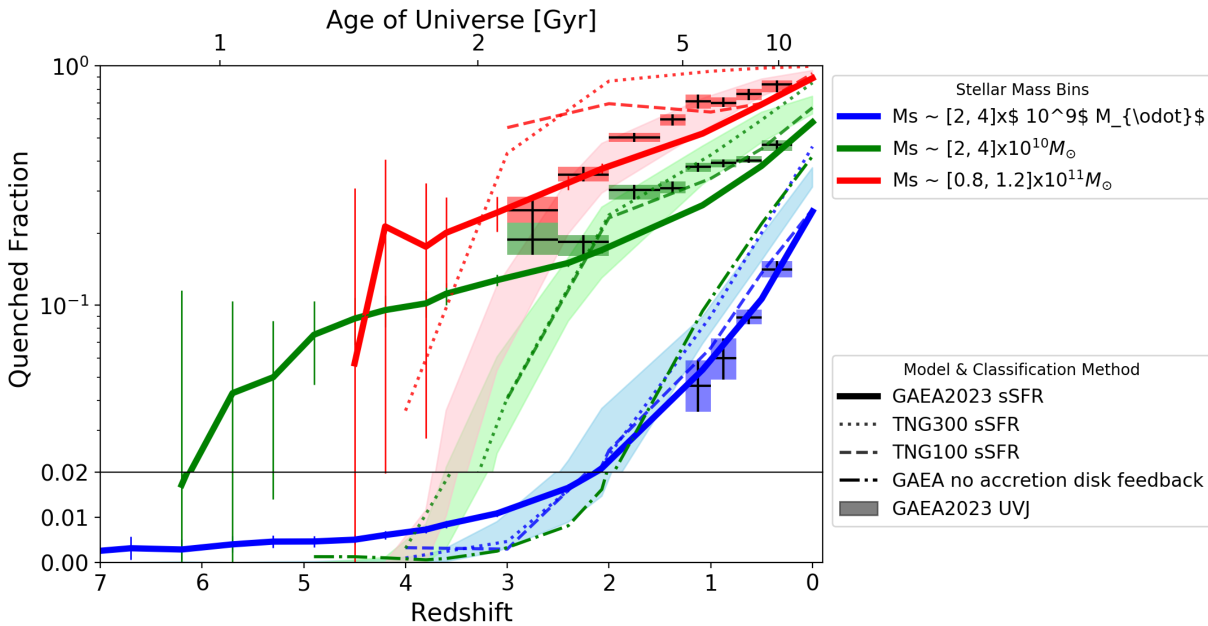

Figure 1. Quenched fractions as a function of redshift. Different colors represent galaxies of different stellar mass. Vertical error bars show the standard deviations obtained for 100 randomly selected sub-samples. Shaded regions show the uncertainties in quiescent fractions from slightly different cuts in the UVJ diagram (more details in text). The dash-dotted line shows results from a GAEA run where accretion disk feedback is switched off. Dotted and dashed lines show the quenched fractions measured from TNG300 and TNG100. Error boxes are observed quenched fractions for UltraVISTA DR1 and 3D-HST survey from Martis et al. (2016).

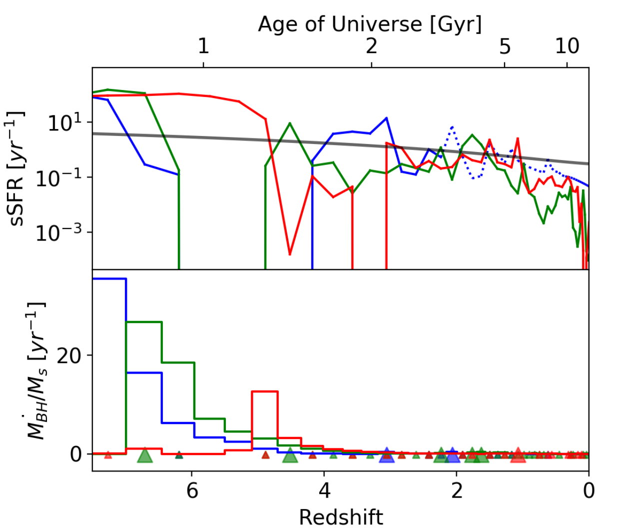

Figure 2. Evolution of three representative galaxies. The upper and lower panels show the evolution of sSFR and the SMBH accretion rate associated with the disk accretion mode normalized by stellar mass. The sSFR is indicated by solid and dotted lines when a galaxy is classified as central or satellite, respectively. The gray straight line in the upper panel is the separation between quenched and star-forming galaxies. Large and small triangles in the lower panel indicate merger events with mass ratios above 0.3 and 0.01. Color code is the same as in Figure 1.

Broadly speaking, we can consider two quenching scenarios: internal quenching, i.e. AGN feedback and SN feedback, and external quenching, i.e. environmental stripping and galaxy-galaxy interactions. In this section, we analyze the relative importance of these quenching mechanisms at different redshifts in the GAEA framework.

First of all, we traced the history of high-redshift quenched galaxies in the three stellar mass ranges considered. Figure 2 shows the evolution histories of three representative galaxies selected from each stellar mass bin. We find that all quenched model galaxies have experienced high-rate black hole accretion and suffered accretion disk feedback right before quenching, suggesting that this mechanism is the main quenching channel at this redshift. This is confirmed by the dot-dashed lines in Figure 1, showing predictions for Milky Way mass galaxies from the a version of GAEA (Xie et al. 2020) that does not include disk accretion feedback and that significantly under-predicts the fractions of quenched galaxies at high redshift (see also in De Lucia et al. 2024).

Since the large accretion rates give rise to luminous quasars, in the top panel of Figure 3 we compare the fraction of quasar-host galaxies in recently-quenched galaxies (dashed) and the entire population (solid). About 70 and 40 per cent of massive and Milky

Way mass galaxies host AGN with bolometric luminosity brighter than 10^{44} erg/s at $z > 2$. These fractions rise to 100 per cent for recently quenched galaxies at $z > 2$. Surprisingly, more than 75% of low-mass quenched galaxies at $z > 2$ also host luminous AGN, whereas the fraction is only 20 per cent for all galaxies in this mass range. The elevated fraction of luminous AGN for quenched galaxies confirms that the disk accretion feedback from SMBH is the dominant quenching mechanism for high redshift galaxies. The fraction of luminous AGN decreases at lower redshift, and the differences between all galaxies and quenched samples also reduce: at low redshift, accretion disk feedback is less important for quenching.

The disk accretion feedback is triggered by both disk instabilities and mergers. While tracing evolution of individual galaxies, we find the large accretion rates are associatd with merger events for Milky Way mass and massive galaxies. In the middle panel of Figure 3 we show the fraction of galaxies that just experienced mergers between the recently quenched and in the entire population. All mergers with a mass ratio larger than 1 : 100 are considered, motivated by the rapid growth of black holes driven by multiple minor mergers or even very minor mergers, which we find to be common for high-z quiescent galaxies. Compared to the entire sample of Milky Way mass and massive galaxies, newly quenched galaxies have much higher merger rates, especially at high redshift. Therefore, mergers represent the main channel for black hole accretion at these mass ranges in the GAEA framework.

For low-mass galaxies, more than half of the recently quenched galaxies haven't experienced any mergers around the time of quenching. We thus conclude that their SMBH accretion are not primarily driven by mergers. We find that low-mass galaxies are more likely to have unstable disks at high redshift, and it is this disk instability that triggers efficient black hole accretion.

The connection between the quenching process and black hole accretion becomes weaker at lower redshift, where environmental effects become increasingly important. The bottom panel of Figure 3 shows the fraction of galaxies that are satellites. In GAEA2023, satellite galaxies lose hot gas and cold gas gradually by tidal stripping and ram-pressure stripping, whereas central galaxies are unaffected. For low-mass galaxies, a larger fraction of satellite galaxies are quenched at as early as $z \sim 6$, so the dependence of quenching on the environment starts at very early epochs in the framework of our model. The phenomenon of environmental quenching starts since $z \sim 3$ for Milky-Way-mass galaxies. The difference in satellite fraction between quenched and all massive galaxies is negligible, which is consistent with previous results that massive galaxies are mainly quenched by AGN feedback (Xie et al. 2020).

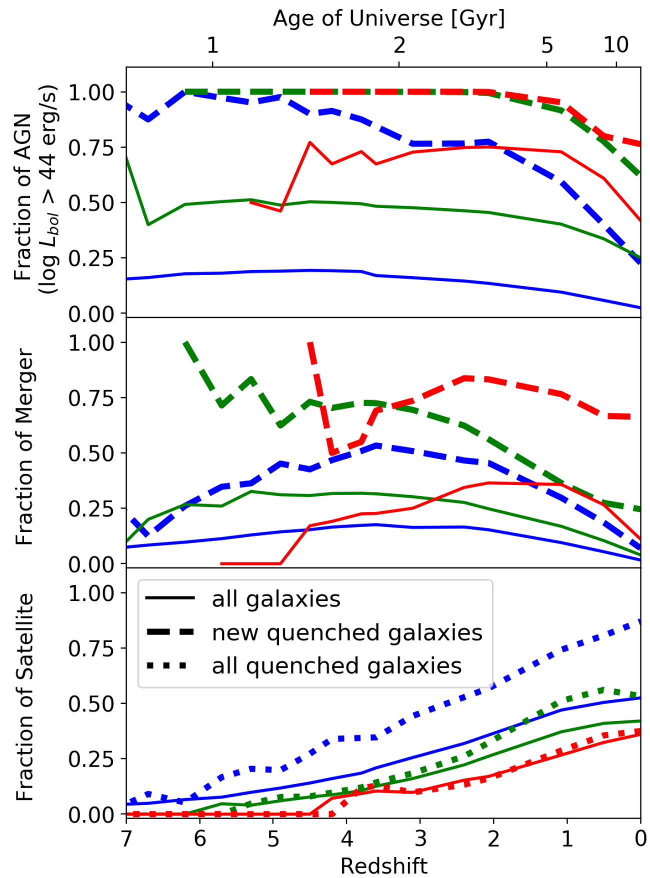

Figure 3. The top, middle, and bottom panels show the fraction of galaxies hosting luminous AGN ($\log L_{bol}/(\mathrm{erg/s}) > 44$), the fraction of galaxies that have experienced recent mergers with a mass ratio larger than 1/100, and the fraction of satellites, respectively. Solid, dotted, and dashed lines correspond to the total, quenched, and newly-quenched galaxy populations, respectively. Color code is the same as in Figure 1.

4. CONCLUSION

In this work we use the semi-analytic model GAEA2023 to study the quenched fractions predicted for massive ($M_\star \sim 10^{11}\mathrm{M}_\odot$), Milky Way mass ($M_\star \sim 10^{10.5}\mathrm{M}_\odot$), and low mass galaxies ($M_\star \sim 10^{9.5}\mathrm{M}_\odot$) since $z = 7$. GAEA2023 predictions are in good agreement with the observed quenched fraction measured from UltraVista and 3D-HST in the redshift range $0 < z < 3$.

The quenched fractions defined by UVJ color are consistent with those defined by sSFR up to $z \sim 3$. At higher redshift, the quenched fractions are underestimated by a UVJ color selection. When adopting a sSFR selection, about 5% of massive galaxies are found to be quenched at $z \sim 4.5$, about 2% of Milky Way mass galaxies are firstly found to be quenched at $z \sim 6.2$, and the quenched fraction of low-mass galaxies is 0.2% at $z \sim 7$. More than half of galaxies are not temporarily quenched due to bursty star formation episodes, as they maintain a low star formation rate for over ~ 1 Gyr.

Taking advantage of our model, we analyse the quenching mechanism at different redshifts. We find that all recently quenched Milky Way and massive galaxies, and more than 75 per cent of low mass newly quenched galaxies at $z > 2$ host luminous quasars (with bolometric luminosity brighter than 10^{44} erg/s). This suggests that accretion disk feedback from SMBHs is the main reason for quenching at high redshift. This is also confirmed by analysing predictions from an alternative model where this physical process is switched off. We find that disk accretion feedback responsible for quenching is driven by galaxy mergers for massive and Milky Way mass galaxies, and by disk instabilities for lower mass galaxies. Environmental effects become increasingly important for low-mass galaxies at $z < 6$, and for Milky Way mass galaxies at $z < 2$. Massive galaxies are not quenched by environmental effects(Hirschmann et al. 2016; De Lucia et al. 2019).

The earliest quenched galaxy so far is at $z \sim 7$ (Looser et al. 2023), and it has a stellar mass of $M_\star \sim 5 \times 10^8 \mathrm{M}_\odot$. At $z \sim 5$, most quenched galaxies discovered are massive galaxies. Based on predictions from our model, we expect to find non-negligible numbers of quenched galaxies with stellar mass $\sim 10^{9.5}\mathrm{M}_\odot$ at $z \sim 7$ or even higher redshift. A large fraction of these galaxies are expected to host liminous quasars.

5. ACKNOWLEDGMENTS

LZX acknowledges support from the National Natural Science Foundation of China (No. 12041302, No. 11903023). We also acknowledge the support of Lorentz Center, ISSI and the use of their facilities, which facilitated discussions on this project. BV acknowledges the support from the INAF Mini Grant 2022 "Tracing filaments through cosmic time" (PI Vulcani). MLB acknowledges support from an NSERC Discovery Grant. GHR acknowledges support from NSF Astronomy and Astrophysics grant 2206473, HST grant GO-16300.004-A, and NASA ADAP grant 80NSSC19K0592. GW gratefully acknowledges support from the National Science Foundation through grant AST-2205189 and from HST program number GO-16300. YMB gratefully acknowledges funding from the Netherlands Organization for Scientific Research (NWO) under Veni grant number 639.041.751 and financial support from the Swiss National Science Foundation (SNSF) under funding reference 200021_213076.

REFERENCES

Alberts, S., Williams, C. C., Helton, J. M., et al. 2023, arXiv e-prints, arXiv:2312.12207, doi: 10.48550/arXiv.2312.12207

Antwi-Danso, J., Papovich, C., Esdaile, J., et al. 2023, arXiv e-prints, arXiv:2307.09590, doi: 10.48550/arXiv.2307.09590

Carnall, A. C., McLure, R. J., Dunlop, J. S., et al. 2023a, Nature, 619, 716, doi: 10.1038/s41586-023-06158-6

Carnall, A. C., McLeod, D. J., McLure, R. J., et al. 2023b, MNRAS, 520, 3974, doi: 10.1093/mnras/stad369

Cecchi, R., Bolzonella, M., Cimatti, A., & Girelli, G. 2019, ApJL, 880, L14, doi: 10.3847/2041-8213/ab2c80

De Lucia, G., Fontanot, F., Xie, L., & Hirschmann, M. 2024, arXiv e-prints, arXiv:2401.06211, doi: 10.48550/arXiv.2401.06211

De Lucia, G., Hirschmann, M., & Fontanot, F. 2019, MNRAS, 482, 5041, doi: 10.1093/mnras/sty3059

De Lucia, G., Tornatore, L., Frenk, C. S., et al. 2014, MNRAS, 445, 970, doi: 10.1093/mnras/stu1752

Dekel, A., Sarkar, K. C., Birnboim, Y., Mandelker, N., & Li, Z. 2023, MNRAS, 523, 3201, doi: 10.1093/mnras/stad1557

Finkelstein, S. L., Leung, G. C. K., Bagley, M. B., et al. 2023, arXiv e-prints, arXiv:2311.04279, doi: 10.48550/arXiv.2311.04279

Fontanot, F., De Lucia, G., Hirschmann, M., et al. 2020, MNRAS, 496, 3943, doi: 10.1093/mnras/staa1716

Forrest, B., Marsan, Z. C., Annunziatella, M., et al. 2020, ApJ, 903, 47, doi: 10.3847/1538-4357/abb819

Franx, M., van Dokkum, P. G., Förster Schreiber, N. M., et al. 2008, ApJ, 688, 770, doi: 10.1086/592431

Gelli, V., Salvadori, S., Ferrara, A., & Pallottini, A. 2023, arXiv e-prints, arXiv:2310.03065, doi: 10.48550/arXiv.2310.03065

Girelli, G., Bolzonella, M., & Cimatti, A. 2019, A&A, 632, A80, doi: 10.1051/0004-6361/201834547

Glazebrook, K., Schreiber, C., Labbé, I., et al. 2017, Nature, 544, 71, doi: 10.1038/nature21680

Gould, K. M. L., Brammer, G., Valentino, F., et al. 2023, AJ, 165, 248, doi: 10.3847/1538-3881/accadc

Hirschmann, M., De Lucia, G., & Fontanot, F. 2016, MNRAS, 461, 1760, doi: 10.1093/mnras/stw1318

Ilbert, O., McCracken, H. J., Le Fèvre, O., et al. 2013, A&A, 556, A55, doi: 10.1051/0004-6361/201321100

Ito, K., Tanaka, M., Miyaji, T., et al. 2022, ApJ, 929, 53, doi: 10.3847/1538-4357/ac5aaf

Kakimoto, T., Tanaka, M., Onodera, M., et al. 2023, arXiv e-prints, arXiv:2308.15011, doi: 10.48550/arXiv.2308.15011

Kimmig, L. C., Remus, R.-S., Seidel, B., et al. 2023, arXiv e-prints, arXiv:2310.16085, doi: 10.48550/arXiv.2310.16085

Kubo, M., Nagao, T., Uchiyama, H., et al. 2024, MNRAS, 527, 403, doi: 10.1093/mnras/stad3210

Kubo, M., Umehata, H., Matsuda, Y., et al. 2021, ApJ, 919, 6, doi: 10.3847/1538-4357/ac0cf8

Kurinchi-Vendhan, S., Farcy, M., Hirschmann, M., & Valentino, F. 2023, arXiv e-prints, arXiv:2310.03083, doi: 10.48550/arXiv.2310.03083

Lagos, C. D. P., Bravo, M., Tobar, R., et al. 2023, arXiv e-prints, arXiv:2309.02310, doi: 10.48550/arXiv.2309.02310

Looser, T. J., D'Eugenio, F., Maiolino, R., et al. 2023, arXiv e-prints, arXiv:2302.14155, doi: 10.48550/arXiv.2302.14155

Lovell, C. C., Roper, W., Vijayan, A. P., et al. 2023, MNRAS, 525, 5520, doi: 10.1093/mnras/stad2550

Marinacci, F., Vogelsberger, M., Pakmor, R., et al. 2018, MNRAS, 480, 5113, doi: 10.1093/mnras/sty2206

Marsan, Z. C., Muzzin, A., Marchesini, D., et al. 2022, ApJ, 924, 25, doi: 10.3847/1538-4357/ac312a

Martis, N. S., Marchesini, D., Brammer, G. B., et al. 2016, ApJL, 827, L25, doi: 10.3847/2041-8205/827/2/L25

McConachie, I., Wilson, G., Forrest, B., et al. 2022, ApJ, 926, 37, doi: 10.3847/1538-4357/ac2b9f

Merlin, E., Fortuni, F., Torelli, M., et al. 2019, MNRAS, 490, 3309, doi: 10.1093/mnras/stz2615

Muzzin, A., Marchesini, D., Stefanon, M., et al. 2013, ApJ, 777, 18, doi: 10.1088/0004-637X/777/1/18

Naiman, J. P., Pillepich, A., Springel, V., et al. 2018, MNRAS, 477, 1206, doi: 10.1093/mnras/sty618

Nanayakkara, T., Glazebrook, K., Jacobs, C., et al. 2022, arXiv e-prints, arXiv:2212.11638, doi: 10.48550/arXiv.2212.11638

Nelson, D., Pillepich, A., Springel, V., et al. 2018, MNRAS, 475, 624, doi: 10.1093/mnras/stx3040

Pillepich, A., Springel, V., Nelson, D., et al. 2018, MNRAS, 473, 4077, doi: 10.1093/mnras/stx2656

Planck Collaboration, Ade, P. A. R., Aghanim, N., et al. 2016, A&A, 594, A13, doi: 10.1051/0004-6361/201525830

Qin, Y., Mutch, S. J., Duffy, A. R., et al. 2017, MNRAS, 471, 4345, doi: 10.1093/mnras/stx1852

Schreiber, C., Glazebrook, K., Nanayakkara, T., et al. 2018, A&A, 618, A85, doi: 10.1051/0004-6361/201833070

Shimakawa, R., Pérez-Martínez, J. M., Koyama, Y., et al. 2023, arXiv e-prints, arXiv:2306.06392, doi: 10.48550/arXiv.2306.06392

Spergel, D. N., Verde, L., Peiris, H. V., et al. 2003, ApJS, 148, 175, doi: 10.1086/377226

Springel, V., White, S. D. M., Jenkins, A., et al. 2005, Nature, 435, 629, doi: 10.1038/nature03597

Springel, V., Pakmor, R., Pillepich, A., et al. 2018, MNRAS, 475, 676, doi: 10.1093/mnras/stx3304

Tanaka, M., Onodera, M., Shimakawa, R., et al. 2023, arXiv e-prints, arXiv:2311.11569, doi: 10.48550/arXiv.2311.11569

Trinca, A., Schneider, R., Valiante, R., et al. 2023, arXiv e-prints, arXiv:2305.04944, doi: 10.48550/arXiv.2305.04944

Valentino, F., Tanaka, M., Davidzon, I., et al. 2020, ApJ, 889, 93, doi: 10.3847/1538-4357/ab64dc

Valentino, F., Brammer, G., Gould, K. M. L., et al. 2023, ApJ, 947, 20, doi: 10.3847/1538-4357/acbefa

Wang, Y.-Y., Lei, L., Yuan, G.-W., & Fan, Y.-Z. 2023, ApJL, 954, L48, doi: 10.3847/2041-8213/acf46c

Weaver, J. R., Davidzon, I., Toft, S., et al. 2023, A&A, 677, A184, doi: 10.1051/0004-6361/202245581

Whitaker, K. E., Labbé, I., van Dokkum, P. G., et al. 2011, ApJ, 735, 86, doi: 10.1088/0004-637X/735/2/86

Williams, R. J., Quadri, R. F., Franx, M., van Dokkum, P., & Labbé, I. 2009, ApJ, 691, 1879, doi: 10.1088/0004-637X/691/2/1879

Wuyts, S., Labbé, I., Förster Schreiber, N. M., et al. 2008, ApJ, 682, 985, doi: 10.1086/588749

Xie, L., De Lucia, G., Hirschmann, M., & Fontanot, F. 2020, MNRAS, 498, 4327, doi: 10.1093/mnras/staa2370

Xie, L., De Lucia, G., Hirschmann, M., Fontanot, F., & Zoldan, A. 2017, MNRAS, 469, 968, doi: 10.1093/mnras/stx889